

Article

An Improved Flexible Solar Thermal Energy Integration Process for Enhancing the Coal-Based Energy Efficiency and NO_x Removal Effectiveness in Coal-Fired Power Plants under Different Load Conditions

Yu Han ^{1,2}, Cheng Xu ^{1,*}, Gang Xu ^{1,*}, Yuwen Zhang ²  and Yongping Yang ¹

¹ Beijing Key Laboratory of Emission Surveillance and Control for Thermal Power Generation, North China Electric Power University, Beijing 102206, China; hanyu900221@163.com (Y.H.); yyp@ncepu.edu.cn (Y.Y.)

² Department of Mechanical & Aerospace Engineering, University of Missouri, Columbia, MO 65211, USA; zhangyu@missouri.edu

* Correspondence: xucheng@ncepu.edu.cn (C.X.); xgncepu@163.com (G.X.)

Received: 8 August 2017; Accepted: 18 September 2017; Published: 25 September 2017

Abstract: An improved flexible solar-aided power generation system (SAPG) for enhancing both selective catalytic reduction (SCR) de-NO_x efficiency and coal-based energy efficiency of coal-fired power plants is proposed. In the proposed concept, the solar energy injection point is changed for different power plant loads, bringing about different benefits for coal-fired power generation. For partial/low load, solar energy is beneficially used to increase the flue gas temperature to guarantee the SCR de-NO_x effectiveness as well as increase the boiler energy input by reheating the combustion air. For high power load, solar energy is used for saving steam bleeds from turbines by heating the feed water. A case study for a typical 1000 MW coal-fired power plant using the proposed concept has been performed and the results showed that, the SCR de-NO_x efficiency of proposed SAPG could increase by 3.1% and 7.9% under medium load and low load conditions, respectively, as compared with the reference plant. The standard coal consumption rate of the proposed SAPG could decrease by 2.68 g/kWh, 4.05 g/kWh and 6.31 g/kWh for high, medium and low loads, respectively, with 0.040 USD/kWh of solar generated electricity cost. The proposed concept opens up a novel solar energy integration pattern in coal-fired power plants to improve the pollutant removal effectiveness and decrease the coal consumption of the power plant.

Keywords: solar aided power generation; selective catalytic reduction (SCR) de-NO_x; coal consumption; solar generated electricity cost; various loads

1. Introduction

Coal is the primary energy source for electricity production, and this will continue for a long period in the future [1]. However, as the major emitters of NO_x, SO_x, dust and CO₂, coal-fired power plant have negative effects on the environment. Using environmentally-friendly alternative energy sources is an effective way to reduce pollutant emissions.

As a good fossil fuel replacement, solar energy has attracted great attention amongst the R&D and industry communities. However, its instability, relatively low intensity and high investment nature constrain the commercial application of solar thermal energy. Integrating solar energy into coal-fired power plants, normally referred to solar-aided power generation (SAPG), offers better performance and lower cost [2]. SAPG was first proposed by Zoschak and Wu in 1975 [3]. In recent

years, Yang et al. [4,5] analyzed the influence of regenerative systems with the integration of solar energy and revealed the coupling mechanism of SAPG. Yan et al. [6,7] analyzed the thermal performance of SAPG systems in different coal-fired units, and evaluated the energy-saving effect with multi-level solar energy use. Popov [8] analyzed the influence of inlet and outlet heated water temperature on the energy saving effect of SAPG. Suresh et al. [9] conducted an energy, exergy, environment and economic (4-E) analysis for SAPG power plants to comprehensively evaluate the thermal and economic performance. Zhong et al. [10] proposed an optimized operation strategy of a SAPG system based on the changeable integrate mode and different solar irradiance. Zhai et al. [11,12] evaluated SAPG systems based on thermo-economic structural and life cycle theory. Peng et al. [13] conducted thermodynamic analysis of SAPG systems under variable loads. Bakos et al. [14] proposed to integrate solar energy into a lignite-fired power plant and analyzed the resulting thermal and economic performance. Hou et al. [15] proposed a new evaluation method of the solar contribution in a SAPG system based on exergy analysis. Pierce et al. [16] compared SAPG and stand-alone concentrating solar power, and concluded that SAPG has great performance advantages. Xu et al. [17] proposed a new system based on integrating solar energy into a low-rank coal pre-drying process, which could significantly improve the boiler efficiency.

To the best of our knowledge, in the previous studies solar energy was generally used to decrease the coal consumption and achieve energy savings effects. It seems that improving thermal performance is the sole function of integrated solar energy in coal-fired power plants. As we know, not only thermal performance but also pollutant removal effectiveness is important for coal-fired power generation, but the integration of solar energy to improve pollutant removal efficiency has not drawn any attention.

In most coal-fired power plants, the SCR de-NO_x device is located downstream of the economizer and upstream of the air preheater. Although the temperature of the SCR de-NO_x unit is in the optimal operation range for the base load in coal-fired power plants, it shows a downtrend as the load decreases, and such as, the SCR de-NO_x temperature is always far below the optimal operation range under low load and medium load conditions. It is common for coal-fired power plants to work under low and medium load, especially in China. It should be noted that a parabolic trough-based solar energy system, which is the most commercially available technology, could heat thermal oil to a temperature of around 400 °C [8,17]. The optimal temperature range of selective catalytic reduction (SCR) de-NO_x units in a coal-fired power plant is 340–390 °C [18–20]. High-efficiency SCR de-NO_x could thus be achieved by integrating solar energy to keep the SCR de-NO_x process at an optimal operation temperature. Obviously, the energy level of parabolic trough-based solar energy and SCR de-NO_x are beneficially matched, so the collected solar energy could increase the de-NO_x process temperature to improve the de-NO_x efficiency.

In this paper, a new solar energy integrated system, which could improve both SCR de-NO_x efficiency and coal saving effects under various loads, was proposed. The integration pattern changes for different power loads. The integrated solar energy is used to increase the SCR de-NO_x efficiency and combustion air temperature at low load while it saves extraction steam under high load conditions, thus offering both energy-saving and environmental protection effects. The thermodynamic and economic performance of the proposed system were determined, and the improvement of SCR de-NO_x performance was also discussed.

2. System Proposal

In most coal-fired power plants, the SCR de-NO_x device is placed in the flue between the economizer and the air preheater (AP). Generally, the SCR de-NO_x temperature is in the optimal operation range under full load, but presents a downtrend as the load decreases. Figure 1 illustrates the connection between the temperature and efficiency of a SCR de-NO_x unit based on the operation curve in a typical coal-fired power plant, as reported in [20].

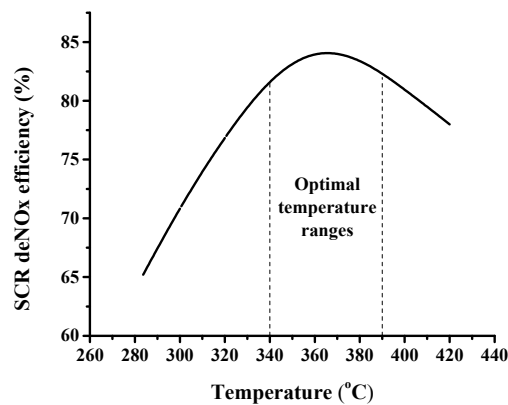


Figure 1. SCR de-NO_x efficiency variation with the temperature.

In order to keep the SCR de-NO_x temperature stable in the optimal operation range, the required solar energy for SCR de-NO_x varies for different loads of a coal-fired unit: (1) no need for high load; (2) a small amount needed for medium load and (3) a large amount needed for low load. Control of the distribution of solar energy under different loads is required, because it is difficult to change the total solar energy collected from collectors with the load variation. One possibility is to use the feed water at the inlet of the No. 1 high pressure regenerative heater (RH) to absorb the extra solar energy under high load and medium load conditions, saving high-pressure extraction steam (No. 1 extraction steam).

Therefore, a novel SAPG system concept for improving both the SCR de-NO_x efficiency and provide coal savings effects is proposed. Figure 2 illustrates the concept of the proposed system for different loads: (1) For a low power load, the solar energy is used to heat the flue gas before the SCR de-NO_x device to increase the SCR de-NO_x temperature up to its optimal operation range, providing a great environmental protection effect (increase of SCR de-NO_x efficiency) as well as additional flue gas heat for preheating the air. The additional flue gas heat, which is obtained from solar energy (injected after the economizer), could be released to the combustion air in the following air preheating process. The additional energy absorbed by the combustion air immediately increases the boiler furnace energy input, which could decrease the coal consumption and bring about a great coal savings effect; (2) For high load, the SCR de-NO_x temperature is in the optimal operation range and does not need to be increased. The collected solar energy is then used to heat the feed water before RH1, saving No. 1 extraction steam. The saved extraction steam could pass through the following stages of the turbines and increase the output power, bringing a great coal savings effect; (3) At medium load, the collected solar energy is used to both heat the flue gas before the SCR de-NO_x device (increasing SCR de-NO_x efficiency as well as increasing the boiler furnace energy input) and heat the feed water before RH1 (saving No. 1 extraction steam).

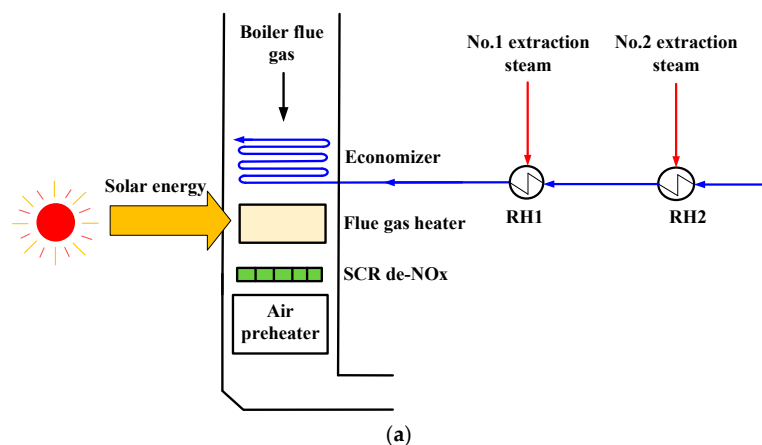


Figure 2. Cont.

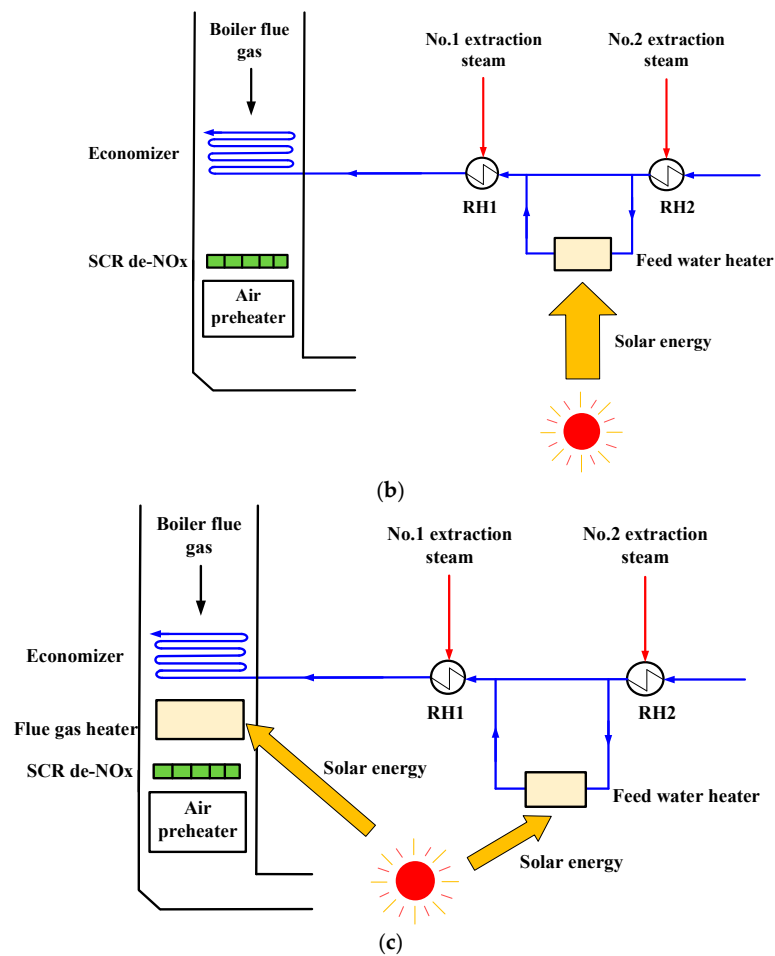


Figure 2. Concept of the proposed SAPG. (a) Low load; (b) High load; (c) Medium load.

3. Application of the Proposed Integrated System in a 1000 MW Coal-Fired Power Plant

3.1. Description of the Reference Plant

A 1000 MW ultra-supercritical coal-fired power plant is selected as a reference case. The live steam is produced at 26.38 MPa and 600 °C, and a single reheater operates at 620 °C and 5.38 MPa. The ultimate and proximate analyses of the raw coal are listed in Table 1. The overall performance of the reference power plant and the main thermal parameters of the regenerative system in design/off-design cases are shown in Tables 2 and 3, respectively. The steam turbine expansion lines on the Mollier diagram of all loads are shown in Figure 3.

Table 1. Proximate analysis of the coal.

Items	M _{ar} (%)	A _{ar} (%)	C _{ar} (%)	H _{ar} (%)	O _{ar} (%)	N _{ar} (%)	S _{ar} (%)	Q _{net,ar} (MJ·kg ⁻¹)
Parameters	18.50	10.24	57.33	3.26	9.43	0.61	0.63	21.23

Table 2. Thermodynamic performance of the reference 1000 MW coal-fired power plant.

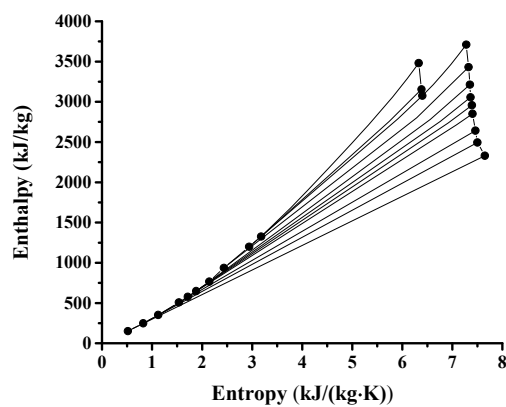
Items	100% (High Load)	75% (Medium Load)	50% (Low Load)
Coal input rate (kg/s)	100.4	76.2	52.4
Total energy of coal input (MW _{th})	2134.3	1619.7	1115.0
Live steam/reheat steam mass flow rate (kg/s)	748.2/620.4	541.8/460.8	354.1/309.2
SCR de-NO _x temperature (°C)	350.0	330.0	311.0

Table 2. Cont.

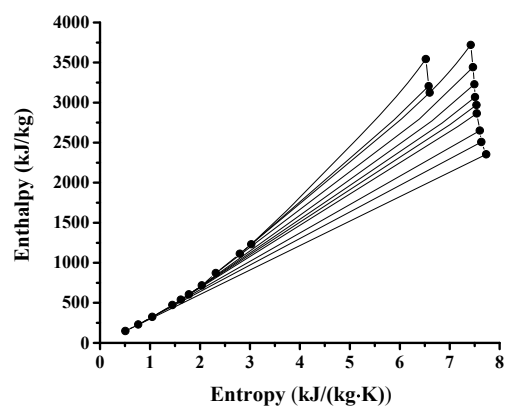
Items	100% (High Load)	75% (Medium Load)	50% (Low Load)
Exhaust flue gas temperature (°C)	121.0	115.0	109.0
Combustion air temperature (°C)	320.0	304.0	290.0
Excess air coefficient	1.15	1.24	1.35
Gross power output (MW)	1000.0	750.0	500.0
Standard coal consumption rate (g/kWh)	262.06	265.17	273.80

Table 3. Primary thermal parameter of the regenerative system of the case unit.

Load	Items	1#	2#	3#	DEA	5#	6#	7#	8#	9#
100% (design load)	Extraction steam temperature (°C)	406.0	359.3	302.5	376.6	297.1	246.4	191.2	88.1	63.2
	Extraction steam pressure (MPa)	8.09	5.78	2.29	1.09	0.60	0.38	0.23	0.07	0.02
	Extraction steam flow rate (kg/s)	40.8	87.0	36.0	23.3	16.5	16.3	31.8	22.6	21.7
	Outlet feed water temperature (°C)	299.2	273.7	216.3	180.6	153.8	137.5	120.8	84.0	59.3
	Outlet feed water pressure (MPa)	32.20	32.21	32.22	1.02	1.02	1.03	1.04	1.05	1.06
	Water flow rate (kg/s)	748.2	748.2	748.2	748.2	561.1	561.1	561.1	496.6	496.6
75% (medium load)	Extraction steam temperature (°C)	411.0	365.0	283.0	382.4	301.5	250.7	196.4	83.2	58.6
	Extraction steam pressure (MPa)	6.05	4.32	1.73	0.84	0.46	0.29	0.18	0.05	0.02
	Extraction steam flow rate (kg/s)	25.2	55.7	25.3	16.81	11.2	11.2	22.5	15.4	13.5
	Outlet feed water temperature (°C)	280.0	255.6	202.2	169.6	143.8	128.5	112.8	77.5	54.7
	Outlet feed water pressure (MPa)	23.81	23.82	23.83	0.78	0.78	0.79	0.80	0.81	0.82
	Water flow rate (kg/s)	541.8	541.8	541.8	541.8	418.7	418.7	418.7	373.9	373.9
50% (low load)	Extraction steam temperature (°C)	416.6	371.5	258.7	388.6	306.3	257.1	202.9	88.1	52.0
	Extraction steam pressure (MPa)	4.07	2.91	1.18	0.59	0.32	0.20	0.12	0.04	0.01
	Extraction steam flow rate (kg/s)	13.5	31.3	15.6	10.6	6.7	6.8	14.2	9.4	6.4
	Outlet feed water temperature (°C)	255.9	233.1	184.4	155.3	130.9	116.7	102.3	68.9	48.1
	Outlet feed water pressure (MPa)	15.97	15.98	15.99	0.55	0.55	0.56	0.57	0.58	0.59
	Water flow rate (kg/s)	354.1	354.1	354.1	354.1	283.0	283.0	283.0	255.3	255.3



(a)



(b)

Figure 3. Cont.

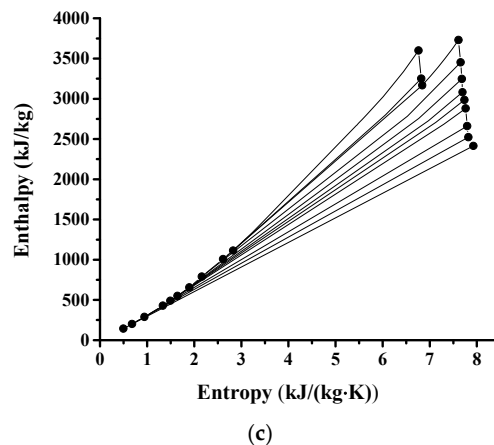


Figure 3. Steam turbine expansion lines on the Mollier diagram of all loads. (a) High load; (b) Medium load; (c) Low load.

3.2. System Description

Figure 4a shows a schematic of the integrated power plant using the proposed concept under different load scenarios. As the most commercially available technology, parabolic trough collectors are used to collect solar energy. An oil-flue gas heater (OFGH) located before the SCR de-NO_x device is adopted to heat the flue gas to increase the SCR de-NO_x temperature for low and medium loads and an oil-water heater (OWH) is used to heat the feed water before RH1 for high and medium loads. A flue gas-air heater (FGAH) is used to recover the extra flue gas heat (increased by the solar energy) and increase the combustion air temperature for low and medium loads. Valves 1 and 2 control the solar energy contribution by controlling the heat conduction oil flow rate for different loads. Valve 3 is used to control the flow rate of feed water. Valves 4 and 5 are employed to control the air flow rate.

1. For a partial load (below 50% of the base load) scenario, valves 1 and 5 open while valves 2–4 close. The schematic of the proposed SAPG is shown in Figure 4b. All the collected solar energy is used to heat the flue gas in the OFGH and the SCR de-NO_x operation temperature increases correspondingly. The additional flue gas heat is recovered in the FGAH and the combustion air temperature is increased.
2. For the baseload, valves 2–4 open while valves 1 and 5 are closed. The schematic of the proposed SAPG is shown in Figure 4c. All the collected solar energy is used to heat the feed water in OWH and save high-grade extraction steam. The SCR de-NO_x temperature is in the optimal operation range and there is no need to increase it, so the OFGH does not work (valve 1 in Figure 4a closes). The FGAH in high load is bypassed and not in operation because there is no additional flue gas heat (valve 5 in Figure 4a closes).
3. For the medium power load, all the valves open and the schematic of the proposed SAPG is shown in Figure 4d. The solar energy is used to heat both the flue gas in OFGH and the feed water in OWH, increasing SCR de-NO_x temperature and saving high-grade extraction steam. Besides, the FGAH is employed to recover the additional flue gas heat, while part of the air is bypassed to keep the exhaust flue gas temperature in a reasonable range.

To evaluate the performance of the proposed SAPG, the following parameters are assumed and designed: (1) For all power loads, the SCR de-NO_x temperatures of the proposed system are kept as 350 °C after integrating solar energy (same as full load); (2) The total collected solar energy is equal to the heat required for SCR de-NO_x at 50% load (low load); (3) The boiler exhaust flue gas temperatures of the proposed SAPG in all loads are same as those of the case unit; (4) The average direct normal irradiation (DNI) of solar energy is set to 0.61 kW/m² (average data in Northwest of China) [2,17].

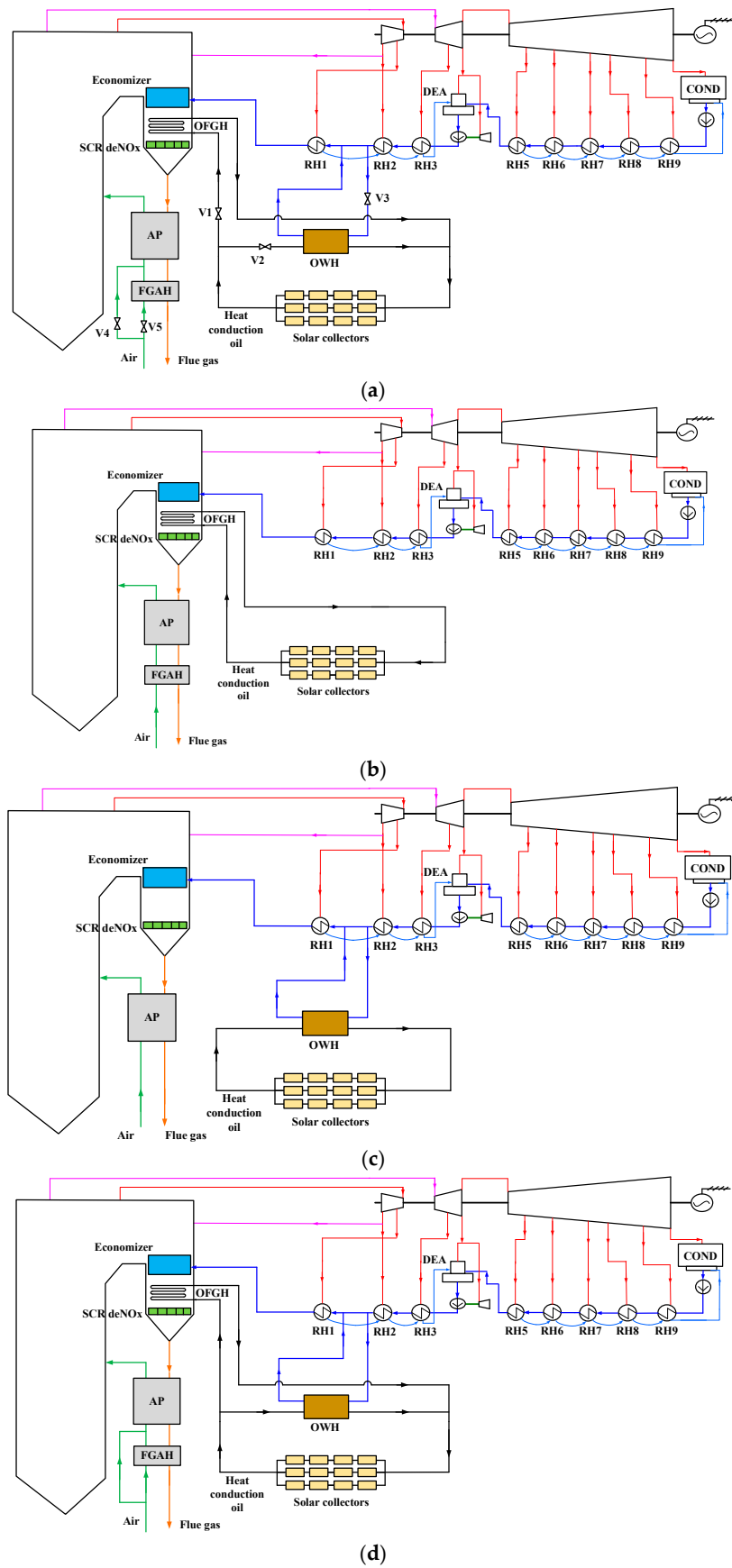


Figure 4. Schematic of the proposed SAPG. (a) Overall schematic; (b) Low load; (c) high load; (d) medium load.

4. Methodology

4.1. Thermodynamic Evaluation

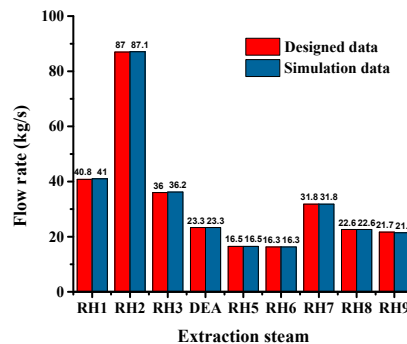
4.1.1. System Simulation

The thermodynamic cycle and energy equilibrium of the proposed SAPG based on the case unit is simulated using the EBSILON Professional software, which is widely used for the design, evaluation and optimization of power plants [21,22]. The model details of the main components are listed in Table 4.

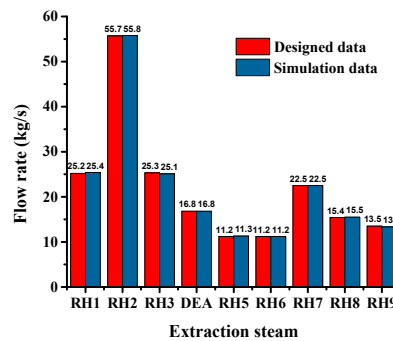
Table 4. Models details of the primary components in EBSILON Professional.

Components	Models
Steam generator	Dry ash extraction and single reheat is modeled as a black box
Steam turbines	Inlet pressure is defined for the steam turbine. In most cases, the outlet pressure is defined by the inlet pressure of the following turbine stage. For the last turbine stage, the outlet pressure is defined by the inlet pressure of the condenser (0.00575 MPa). Mechanical Efficiency = 0.998
RHs	Upper terminal temperature difference and the lower terminal temperature difference of the after-cooler are to be specified. Pressure loss = 3.3–5% in the steam extraction of different RHs, Heat loss = 0%
Condenser	Inlet temperature (20 °C) and pressure (0.1 MPa) of the cooling medium is specified, upper temperature difference = 5 °C, pressure loss = 0.005 Mpa
Pumps	Isentropic efficiencies = 0.8, mechanical efficiency = 0.998
Electric generator	Generator efficiency = 0.99
Solar collector, OFGH, OWH and FGAH	The heat transfer capacity is calculated using the heat balance equation in Section 4.1.1

Figure 5 compares the simulation results and designed data of extraction steam flow rate in the case unit, based on all loads and the designed coal input rate.



(a)



(b)

Figure 5. Cont.

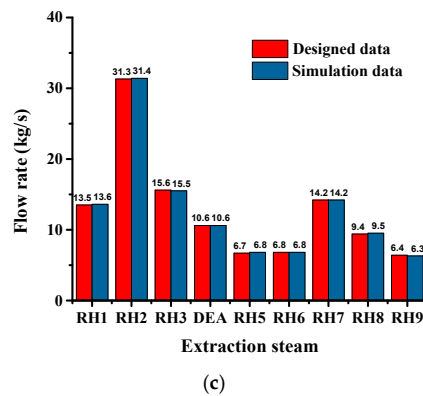


Figure 5. Comparison of the simulation data and designed data of extraction steam flow rate. (a) High load; (b) Medium load; (c) Low load.

The high agreement between the simulated results and the real data proves that the models are reliable to simulate the thermal progress of the proposed SAPG. In order to make the simulation reliable and simple, the solar collector, OFGH, OWH and FGAH are regarded as heat injection sources of the coal-fired power plant. Based on the energy balance, in the proposed SAPG, the required energy for SCR de-NO_x is equal to the additional available flue gas heat for air preheating and the additional heat absorbed by the combustion air, which can be expressed as:

$$Q_{\text{SCR}} = B_j(I_p - I_c) = Q_{\text{fg}} = Q_a = B_j \cdot \alpha_0(I_p^0 - I_c^0) \quad (1)$$

where Q_{fg} and Q_a represent the additional available flue gas heat and the additional heat absorbed by the combustion air (kW). I_p and I_c denote the flue gas enthalpies (kJ/kg-coal) at the SCR de-NO_x temperature of the proposed SAPG (350 °C) and case unit, respectively. I_p^0 and I_c^0 are the theoretical hot air enthalpies (kJ/kg-coal) in the proposed SAPG and the case unit, respectively. B_j represents the coal combustion rate (kg/s) and α_0 denotes the excess air ratio.

The total required solar energy is equal to the sum of required energy for SCR de-NO_x and the heat absorbed by feed water before RH1, which can be expressed as:

$$Q_s = Q_{\text{SCR}} + Q_{\text{RH1}} \quad (2)$$

4.1.2. Heat Transfer Area Calculation

The area of the solar collectors could be calculated as [17]:

$$A_s = \frac{Q_s}{\text{DNI} \cdot \phi} \quad (3)$$

where Q_s denotes the total required solar energy of the proposed SAPG (kW); ϕ is the solar collector efficiency and DNI represents the average direct normal irradiation of solar energy.

The solar collector efficiency ϕ , which is relative to the inlet fluid temperature, ambient air temperature and DNI, could be calculated as [23]:

$$\phi = 73.3 - 0.007276 \cdot \Delta T - 0.496 \cdot \left(\frac{\Delta T}{\text{DNI}}\right) - 0.0691 \cdot \left(\frac{\Delta T^2}{\text{DNI}}\right) \quad (4)$$

where ΔT is receiver fluid temperature above ambient air temperature (°C).

The overall heat transfer coefficient of the FGAH can be given as follows [24]:

$$K_{\text{FGAH}} = \frac{\xi \cdot C_n}{\frac{1}{x_{\text{fg}} \cdot \alpha_{\text{fg}}} + \frac{1}{x_{\text{a1}} \cdot \alpha_{\text{a1}} + x_{\text{a2}} \cdot \alpha_{\text{a2}}}} \quad (\text{W}/(\text{m}^2 \cdot \text{K})) \quad (5)$$

where α_{fg} , α_{a1} and α_{a2} denote the convective heat transfer coefficients of the flue gas, primary air and secondary air, respectively; ζ denotes the utilization factor (0.9); C_n represents the factor reflecting the rotational speed ($C_n = 1$) [24]; and x_{fg} (0.46), x_{a1} (0.14) and x_{a2} (0.28) represent the share of the flue gas, primary air and secondary air in the air preheater, respectively.

The overall heat transfer coefficient of OFGH and OWH can be calculated as follows [25]:

$$K = \frac{1}{\frac{1}{\alpha_1} + \frac{1}{\alpha_2} + R_{th1} + R_{th2}} \quad (6)$$

where α_1 and α_2 denotes the convective heat transfer coefficients of hot source and cold source, respectively. R_{th1} and R_{th2} represents the thermal resistance of the tube wall and fouling thermal resistance, respectively.

The heat transfer area can be calculated as follows:

$$A = \frac{Q}{K \cdot \Delta t} \quad (7)$$

where Q represents the heat transfer capacity and Δt denotes the logarithmic mean temperature difference.

4.2. SCR de-NO_x Performance Evaluation

Operation temperature is the most important parameter in the SCR de-NO_x process of a coal-fired power plant. Generally, the SCR de-NO_x efficiency is high at full load but presents downtrend as the load decreases, which is due to the decreased operation temperature. The increase of the SCR de-NO_x efficiency by incorporating the proposed SAPG is calculated based on the operation curve in a typical coal-fired power plant, which is illustrated in Figure 1 [20]. The total NO_x production could be calculated as follows [26]:

$$G_{NOx} = 1.63B_j \cdot (\beta \cdot N_{ar} + V_y \cdot 10^{-6} \cdot C_{NOx}) \quad (8)$$

where β represents the transform ratio of fuel-nitrogen to NO_x; V_y denotes the flue gas flow rate (m³/kg-coal); and C_{NOx} is the thermal NO_x produced by coal (m³/kg-coal).

4.3. Briefly Economic Evaluation

To evaluate the economic performance of the proposed SAPG, the cost of the generated electric power possible after introducing the solar energy is selected as the evaluation criteria and the cost of electricity (COE) is calculated as [17,21]:

$$COE = \frac{FCI \cdot CRF + O\&M}{E_s} \quad (9)$$

where O&M represents the annual operating and maintenance costs; E_s is the additional solar electricity output, which is equal to the electricity output increase of the proposed SAPG.

The capital recovery factor (CRF) can be calculated as [17,27]:

$$CRF = \frac{(1+r)^n \cdot r}{(1+r)^n - 1} \quad (10)$$

where r denotes the discount rate and n represents the expected plant lifetime.

The fixed capital investment (FCI) of the solar collecting device and FGAIH can be calculated using the scaling up method, which is expressed as [17,27]:

$$FCI = FCI_r \cdot \left(\frac{S}{S_r}\right)^f \quad (11)$$

where FCI_r is the reference FCI of the equipment; S and S_r denote the scale parameter of the equipment in the proposed SAPG and the reference equipment, respectively; f is the scaling factor.

The main parameters for COE and FCI calculations are shown in Tables 5 and 6, which can be obtained from [2,17,28–31].

Table 5. Basic parameters for economic analysis.

Items	Values
Annual effective interest rate (r)	8%
Plant economic life (n)	25 years
O&M	4% of FCI
Annual operating hours	3037 h/year
Annual high load (100%) operating hours	1263 h/year
Annual medium load (75%) operating hours	1120 h/year
Annual low load (50%) operating hours	1867 h/year

Table 6. Basic capital cost data of facilities.

Component	Reference FCI (Million USD)	Reference Scale	Scale Unit	Scaling Factor
Solar collector	34.78	186,000	Area (m ²)	0.90
OFGH	0.69	13,149	Heat transfer area (m ²)	0.68
OWH	0.80	8372	Heat transfer area (m ²)	0.68
FGAH	6.24	353,949	Heat transfer area (m ²)	0.68

5. Results and Discussion

5.1. Thermal Performance

Table 7 shows the parameters of the main heat exchangers in the proposed SAPG. The following observations are obtained from Table 7: (1) In the proposed SAPG, the total collected solar energy in all loads is 24.5 MW_{th}; (2) the utilization of 24.5 MW_{th} of solar energy varies in different load; and (3) the heat transfer area of all heat exchangers is not large, which is reasonable and practical in engineering.

Table 7. Thermal parameters of the primary heat exchangers in the proposed SAPG.

Heat Exchangers	Items	100% (High Load)	75% (Medium Load)	50% (Low Load)
Solar collector	Inlet/outlet oil temperature (°C)	380.0/338.0	380.0/338.0	380.0/338.0
	Oil flow rate (kg/s)	244.0	244.0	244.0
	Efficiency	70.8	70.8	70.8
	Heat transfer capacity (MW _{th})	24.5	24.5	24.5
	Heat transfer area (m ²)	56,729	56,729	56,729
OFGH	Inlet/outlet oil temperature (°C)	-/-	380.0/338.0	380.0/338.0
	Inlet/outlet flue gas temperature (°C)	-/-	330.0/350.0	311.0/350.0
	Oil/flue gas flow rate (kg/s)	-/-	169.3/761.6	244.0/566.6
	Overall heat transfer coefficient (W/m ² K)	-	40.0	33.7
	Heat transfer capacity (MW _{th})	-	17.0	24.5
OWH	Inlet/outlet oil temperature (°C)	380.0/338.0	380.0/338.0	-/-
	Inlet/outlet feed water temperature (°C)	273.7/280.6	255.6/349.9	-/-
	Oil/water flow rate (kg/s)	244.0/745.7	74.7/15.4	-/-
	Overall heat transfer coefficient (W/m ² K)	279.6	132.8	-
	Heat transfer capacity (MW _{th})	24.5	7.5	-
FGAH	Inlet/outlet flue gas temperature (°C)	-/-	135.1/115.0	147.5/109.0
	Inlet/outlet air temperature (°C)	-/-	28.8/90.5	34.6/83.1
	Flue gas/air flow rate (kg/s)	-/-	804.5/257.4	607.4/501.5
	Overall heat transfer coefficient (W/m ² K)	-	10.3	13.5
	Heat transfer capacity (MW _{th})	-	17.0	24.5
	Heat transfer area (m ²)	-	26,172	26,172

The thermal performance of the proposed SAPG is illustrated in Table 8. It can be seen that the proposed SAPG could reduce the standard coal consumption rate by 2.68 g/kWh, 4.05 g/kWh and 6.31 g/kWh under high, medium and low load, respectively. The increase of the output electric power varies from 10.4 MW_e to 11.9 MW_e under different loads. In general, the proposed SAPG has a great coal saving effect for all loads. The coal saving effect shows an uptrend with the decrease of load.

Table 8. Thermal performance of the proposed SAPG.

Items	100% (High Load)	75% (Medium Load)	50% (Low Load)
Combustion air temperature increase (°C)	-	28.3	50.6
Saved high-grade extraction steam (kg/s)	12.3	3.2	-
Gross power generated (MW _e)	1010.4	761.7	511.9
Gross additional power generated (MW _e)	10.4	11.7	11.9
Standard coal consumption rate (g/kWh)	259.40	261.11	267.48
Standard coal consumption rate decrease (g/kWh)	2.68	4.05	6.31

Figure 6 compares the coal-based thermal efficiency of the proposed system and the original case unit under different loads. As indicated, the coal-based thermal efficiency of the proposed is 47.34%, 47.03% and 45.01% under high, medium and low load, respectively, which is 0.49%, 0.72% and 1.07% higher than that of the original case unit.

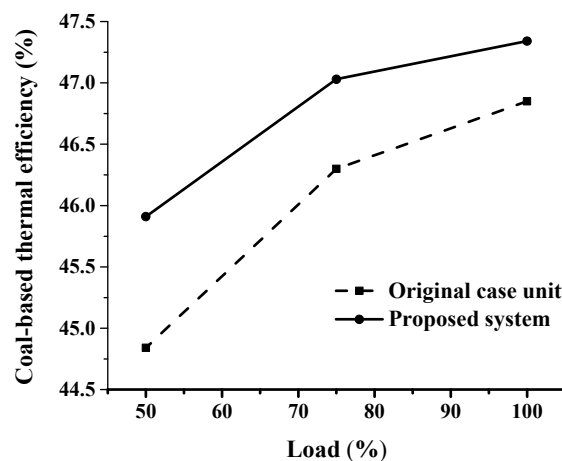


Figure 6. Coal-based thermal efficiency of the proposed system and original case unit.

The energy flow of the proposed SAPG under different loads are illustrated in Figure 7. The following observations can be derived: (1) the solar energy inputs for all loads are the same (24.5 MW_{th}); (2) For high loads, the solar energy enters the regenerative cycle by heating the feed water, which could save 24.5 MW_{th} of heat from the steam turbine bleeds; (3) For low loads, solar energy increases the combustion air temperature, which leads to 24.5 MW_{th} of immediate energy input increase of the boiler and could produce more live steam; (4) For medium loads, 17.0 MW_{th} of solar energy enters the boiler by increasing the combustion air temperature while 7.5 MW_{th} of that enters the regenerative cycle by heating the feed water; (5) Compared with the saved No. 1 extraction steam (406 °C, 8.09 MPa) under high load, the energy level of additional live steam (600 °C, 26.38 MPa) produced by solar energy under low load is higher. Obviously, the energy level of solar energy is upgraded by the new utilization method in low load. It explains why the energy saving effect for low loads is significantly greater than that for high loads.

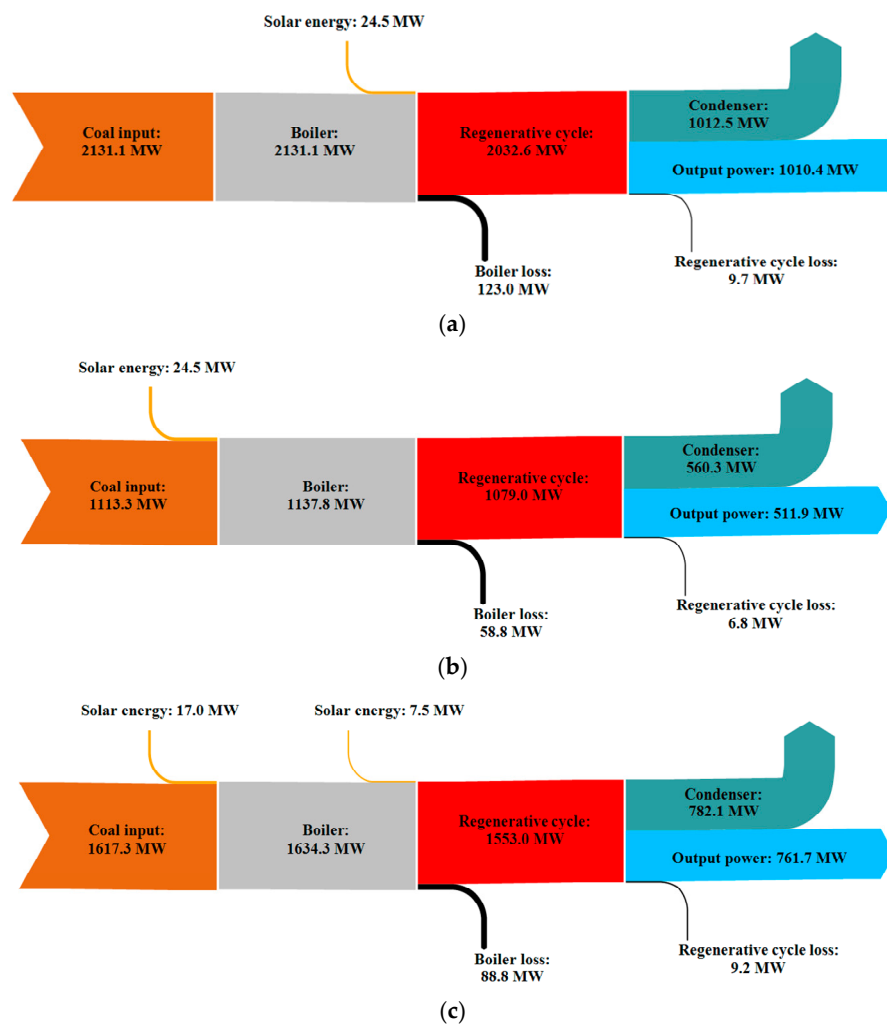


Figure 7. Energy flow of the proposed SAPG. (a) High load; (b) low load; (c) medium load.

5.2. SCR de-NO_x Efficiency Increase

Table 9 illustrates the SCR de-NO_x performance of the proposed SAPG. Figure 8 compares the SCR de-NO_x efficiency in the proposed SAPG and the original case unit. As can be seen, for all loads of the proposed SAPG, the SCR de-NO_x temperature and efficiency are kept at 350 °C and 82.9%, respectively. The SCR de-NO_x efficiency increases by 3.1% and 7.9% under medium load and low load, respectively, as compared with the reference case. In general, the proposed SAPG shows great NO_x removal benefits under low load.

Table 9. SCR de-NO_x performance improvement of the proposed SAPG.

Items	100% (High Load)	75% (Medium Load)	50% (Low Load)
SCR de-NO _x temperature of the referenced unit (°C)	350.0	330.0	311.0
SCR de-NO _x temperature of the proposed SAPG (°C)	350.0	350.0	350.0
SCR de-NO _x temperature increase (°C)	-	20.0	39.0
SCR de-NO _x efficiency of the original case unit (%)	82.9	79.8	75.0
SCR de-NO _x efficiency of the proposed SAPG (%)	82.9	82.9	82.9
SCR de-NO _x efficiency increase (%)	-	3.1	7.9

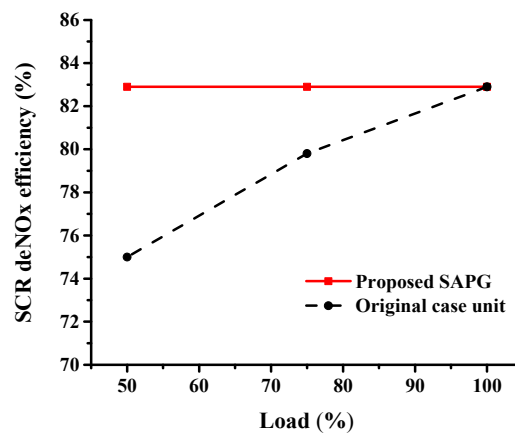


Figure 8. Comparison of the SCR de-NO_x efficiency in the proposed SAPG and original case unit.

Figure 9 illustrates the contribution of NO_x emission decrease in the proposed SAPG. As indicated, the improvement of SCR de-NO_x efficiency could bring 128.7 kg/s and 74.0 kg/s of NO_x emission decrease under low load and medium load, respectively. The NO_x emission decreases caused by coal savings vary from 5.6 kg/s to 9.6 kg/s under different loads. Obviously, the improvement of SCR de-NO_x efficiency provides the main contribution for the NO_x emission decrease at low load and medium load, which accounts for over 90%.

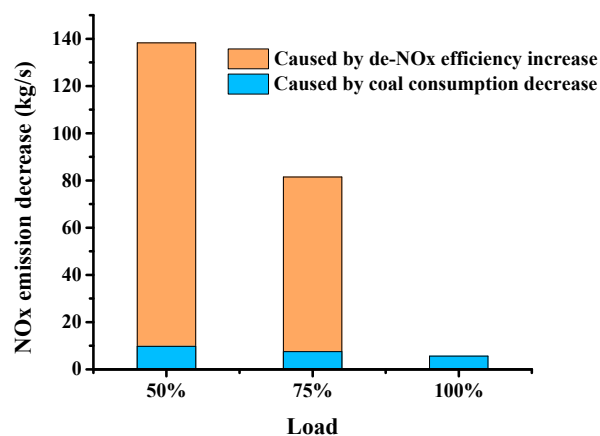


Figure 9. Contribution to NO_x emission decrease in the proposed SAPG.

5.3. Sensitivity Analysis

In the proposed system, the solar intensity will influence the SCR de-NO_x performance and thermal performance. The off-design behavior of the solar field is performed in this section. As we know, the DNI of solar energy may show abrupt changes. In the proposed flexible system, the abrupt changes of DNI could be dealt by controlling the solar energy contribution (by controlling the flow rate of the heat conduction oil by valves). (1) When DNI increases, the additional solar energy is used to heat feed water in all loads, which could bring good energy savings effects; (2) When DNI decreases, the solar energy injected to the feed water decreases first. The solar energy injected to the flue gas will decrease when there is no solar energy in the feed water heating process. The flexible operation mode could weaken the influence of abrupt changes of DNI and keep great SCR de-NO_x performance of the proposed system.

Figure 10 illustrates the variations of the solar energy contribution as a function of changes in solar intensity. The following observation are derived: (1) Under high load, the solar energy for heating feed water shows an uptrend as DNI increases; (2) For medium and low loads, as DNI increases, the solar energy for SCR de-NO_x performance improvement firstly shows an uptrend, and then

remains constant. The solar energy for heating feed water shows an uptrend with the increase of DNI, when DNI is higher than 424 W/m^2 and 610 W/m^2 under medium and low loads, respectively.

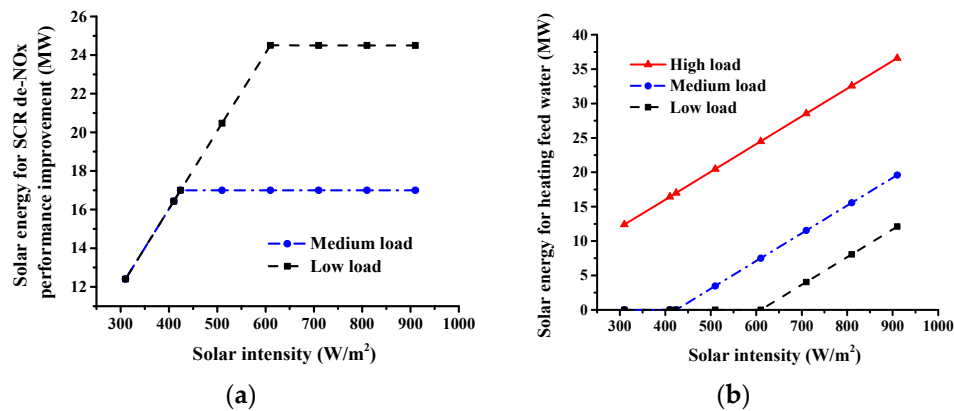


Figure 10. Influence of solar intensity on solar energy contribution. (a) For SCR de-NO_x performance improvement; (b) for heating feed water.

Figure 11 shows the variations of the SCR de-NO_x efficiency and standard coal consumption rate decrease as a function of changes in solar intensity. As indicated in Figure 11, the SCR de-NO_x efficiency of the proposed SAPG at high load remains at 82.9% with the changes of solar intensity. For medium and low load, the SCR de-NO_x efficiency will reduce slightly when the solar intensity is lower than 424 W/m^2 and 610 W/m^2 , respectively. In the point of thermal performance, as the solar intensity increases, the standard coal consumption rate decrease shows an uptrend. In general, under a relatively large variation of solar intensity, the proposed SAPG could keep high SCR de-NO_x efficiency and great energy saving effects for all loads.

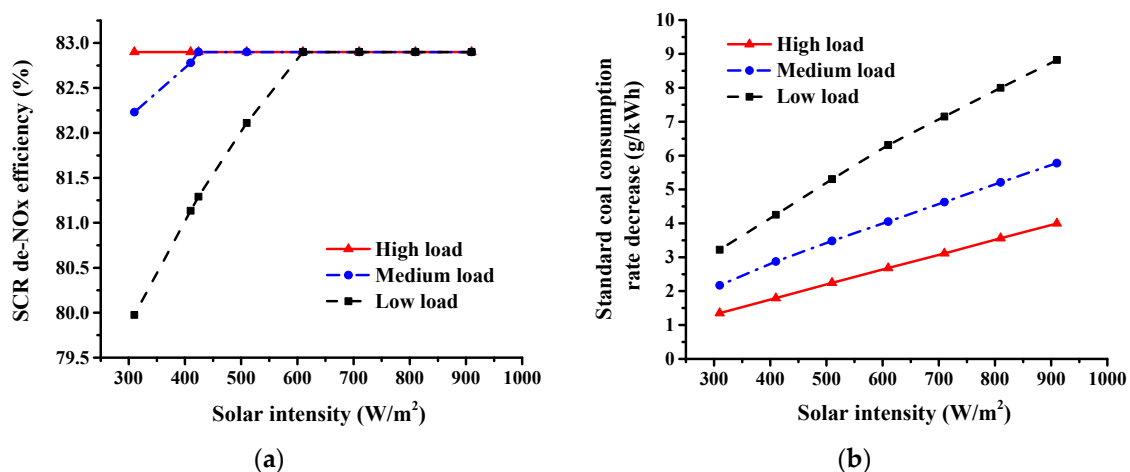


Figure 11. Influence of (a) solar intensity on SCR de-NO_x efficiency and (b) standard coal consumption rate decrease.

5.4. Economic Performance

Table 10 provides the economic performance of the proposed SAPG. As indicated in Table 10, the COE of solar generated electricity is 0.040 USD/kWh, which is lower than the current parabolic trough SAPG (0.09–0.11 USD/kWh) [2,17]. The reasons mainly come from the combined effects of the high coal savings effect and the affordable FCI of the additional equipment.

Table 10. Economic performances of the proposed SAPG.

Items	Proposed SAPG
<i>FCI of the additional equipment</i>	
Solar collector (million USD)	11.95
OFGH (million USD)	1.08
OWH (million USD)	0.21
FGAH (million USD)	1.06
Total additional FCI (million USD)	14.3
Additional operation and maintenance cost (million USD)	0.57
Additional solar electricity output (GWh)	48.5
COE of solar generated electricity (USD/kWh)	0.040

6. Conclusions

An improved flexible solar-aided power generation system (SAPG) for enhancing both the selective catalytic reduction (SCR) de-NO_x efficiency and coal-based energy efficiency of coal-fired power plants under different power loads was proposed. This opens up a novel solar energy integration pattern in solar-aid coal-fired power plants. The SCR de-NO_x efficiency of the proposed SAPG could increase by 3.1% and 7.9% under medium load and low load, respectively, by integrating the solar energy to increase the operation temperature of SCR de-NO_x. Under high load, the proposed SAPG could reduce the standard coal consumption rate by 2.68 g/kWh by heating the feed water, and under low load, 6.31 g/kWh of standard coal consumption rate is reduced by reheating the combustion air. Under medium load, both the combustion air and feed water are heated and the resulting reduction of standard coal consumption is 4.05 g/kWh.

Acknowledgments: This study was partially supported by the National Major Fundamental Research Program of China (No. 2015CB251504), the National Nature Science Fund of China (No. 51706065, No. 51476053) and the Fundamental Research Funds for the Central Universities (No. 2017MS013, No. 2017ZZD003, No. 2015XS78).

Author Contributions: For research articles with several authors, a short paragraph specifying their individual contributions must be provided. Yu Han proposed the original ideas, carried out simulation, conducted calculation and wrote the paper. Cheng Xu, Gang Xu and Yuwen Zhang checked the paper, revised the paper and provided language support. Cheng Xu, Gang Xu and Yongping Yang provided technical and financial support.

Conflicts of Interest: The authors declare no conflict of interest.

Nomenclature

Abbreviations:	Full name
AP	Air preheater
COE	Cost of electricity
COND	Condenser
CRF	Capital recovery factor
DEA	Deaerator
DNI	Direct normal irradiation
FCI	Fixed capital investment
FGAH	Flue gas-air heater
OFGH	Oil-flue gas heater
OWH	Oil-water heater
RH	Regenerative heater
SAPG	Solar aided power generation
SCR	Selective catalytic reduction
Symbols:	Content
B_j	Coal combustion rate
C_{NO_x}	Thermal NO _x produced by coal
C_n	Rotational speed factor

E_s	Additional solar electricity output
f	Scale factor
G_{NO_x}	Total produced NO_x
I	Enthalpy of flue gas
I^0	Enthalpy of air
K	Heat transfer coefficient
n	Number of years
O&M	Ratio of annual operating and management
Q	Heat transfer capacity
R_{th}	Thermal resistance
r	Fraction interest rate per year
S	Scale parameter
V_y	Flue gas flow rate
x	Proportion
α	Convective heat transfer coefficients
α_0	Excess air ratio
β	Transform ratio of fuel-nitrogen to NO_x
ζ	Utilization factor
ΔT	Receiver fluid temperature above ambient air temperature
Δt	Logarithmic mean temperature difference
φ	Solar collector efficiency
Subscripts:	Content
a	Air
a1	Primary air
a2	Secondary air
c	Case unit
fg	Flue gas
p	Proposed system
r	Reference device
s	Solar energy

References

- Xu, C.; Xu, G.; Zhao, S.; Zhou, L.; Yang, Y.; Zhang, D. An improved configuration of lignite pre-drying using a supplementary steam cycle in a lignite fired supercritical power plant. *Appl. Energy* **2015**, *160*, 882–891. [[CrossRef](#)]
- Hong, H.; Zhao, Y.; Jin, H. Proposed partial repowering of a coal-fired power plant using low-grade solar thermal energy. *Int. J. Thermodyn.* **2011**, *14*, 21–28.
- Zoschak, R.J.; Wu, S.F. Studies of the direct input of solar energy to a fossil-fueled central station steam power plant. *Sol. Energy* **1975**, *17*, 297–305. [[CrossRef](#)]
- Yang, Y.P.; Cui, Y.H.; Hou, H.J.; Guo, X.Y.; Yang, Z.P.; Wang, N.L. Research on solar aided coal-fired power generation system and performance analysis. *Sci. China Ser. E Technol. Sci.* **2008**, *51*, 1211–1221. [[CrossRef](#)]
- Yang, Y.; Yan, Q.; Zhai, R.; Kouzani, A.; Hu, E. An efficient way to use medium-or-low temperature solar heat for power generation—Integration into conventional power plant. *Appl. Therm. Eng.* **2011**, *31*, 157–162. [[CrossRef](#)]
- Yan, Q.; Hu, E.; Yang, Y.; Zhai, R. Evaluation of solar aided thermal power generation with various power plants. *Int. J. Energy Res.* **2011**, *35*, 909–922. [[CrossRef](#)]
- Yan, Q.; Yang, Y.; Nishimura, A.; Kouzani, A.; Hu, E. Multi-point and multi-level solar integration into a conventional coal-fired power plant. *Energy Fuels* **2010**, *24*, 3733–3738. [[CrossRef](#)]
- Popov, D. An option for solar thermal repowering of fossil fuel fired power plants. *Sol. Energy* **2011**, *85*, 344–349. [[CrossRef](#)]
- Suresh, M.V.J.J.; Reddy, K.S.; Kolar, A.K. 4-E (Energy, exergy, environment, and economic) analysis of solar thermal aided coal-fired power plants. *Energy Sustain. Dev.* **2010**, *14*, 267–279. [[CrossRef](#)]

10. Zhong, W.; Chen, X.; Zhou, Y.; Wu, Y.; López, C. Optimization of a solar aided coal-fired combined heat and power plant based on changeable integrate mode under different solar irradiance. *Sol. Energy* **2017**, *150*, 437–446. [[CrossRef](#)]
11. Zhai, R.; Liu, H.; Li, C.; Zhao, M.; Yang, Y. Analysis of a solar-aided coal-fired power generation system based on thermo-economic structural theory. *Energy* **2016**, *102*, 375–387. [[CrossRef](#)]
12. Zhai, R.; Li, C.; Chen, Y.; Yang, Y.; Patchigolla, K.; Oakey, J.E. Life cycle assessment of solar aided coal-fired power system with and without heat storage. *Energy Convers. Manag.* **2016**, *111*, 453–465. [[CrossRef](#)]
13. Peng, S.; Hong, H.; Wang, Y.; Wang, Z.; Jin, H. Off-design thermodynamic performances on typical days of a 330 MW solar aided coal-fired power plant in China. *Appl. Energy* **2014**, *130*, 500–509. [[CrossRef](#)]
14. Bakos, G.C.; Tsechlidou, C. Solar aided power generation of a 300 MW lignite fired power plant combined with line-focus parabolic trough collectors field. *Renew. Energy* **2013**, *60*, 540–547. [[CrossRef](#)]
15. Hou, H.; Xu, Z.; Yang, Y. An evaluation method of solar contribution in a solar aided power generation (SAPG) system based on exergy analysis. *Appl. Energy* **2016**, *182*, 1–8. [[CrossRef](#)]
16. Pierce, W.; Gauché, P.; Backström, T.V.; Brent, A.C.; Tadros, A. A comparison of solar aided power generation (SAPG) and stand-alone concentrating solar power (CSP): A South African case study. *Appl. Therm. Eng.* **2013**, *61*, 657–662. [[CrossRef](#)]
17. Xu, C.; Bai, P.; Xin, T.; Hu, Y.; Xu, G.; Yang, Y. A novel solar energy integrated low-rank coal fired power generation using coal pre-drying and an absorption heat pump. *Appl. Energy* **2017**, *20*, 170–179. [[CrossRef](#)]
18. Yang, J.; Fan, L.; Zhao, H. Coordinated optimization control of flue gas temperature for improving reaction efficiency of catalyst. *Proc. CSEE* **2014**, *34*, 2244–2250. (In Chinese)
19. Xu, Y.; Zhang, Y.; Wang, J.; Yuan, Y. Application of CFD in the optimal design of a SCR–DeNO_x system for a 300 MW coal-fired power plant. *Comput. Chem. Eng.* **2013**, *49*, 50–60. [[CrossRef](#)]
20. Gao, Y. *Experimental and Mechanism Analysis on Selective Catalytic Reduction DeNO_x Catalyst*; Shandong University: Shandong, China, 2013. (In Chinese)
21. Wang, L.; Yang, Y.; Dong, C.; Morosuk, T.; Tsatsaronis, G. Multi-objective optimization of coal-fired power plants using differential evolution. *Appl. Energy* **2014**, *115*, 254–264. [[CrossRef](#)]
22. Gewald, D.; Karellas, S.; Schuster, A.; Spliethoff, H. Integrated system approach for increase of engine combined cycle efficiency. *Energy Convers. Manag.* **2012**, *60*, 36–44. [[CrossRef](#)]
23. Dudley, V.E.; Kolb, G.J.; Mahoney, A.R.; Mancini, T.R.; Matthews, C.W. *Test Results: SEGS LS-2 Solar Collector*; Sandia National Laboratories: Albuquerque, NM, USA, 1994.
24. Wu, X. *General Methods of Calculation and Design for Industrial Boiler*; Standards Press of China: Beijing, China, 2003. (In Chinese)
25. Liu, J. *Theory and Design for Fin-Tube Heat Exchangers*; Harbin Institute of Technology Press: Harbin, China, 2013. (In Chinese)
26. Wang, M.; Liao, C. Evaluation of nitrogen oxides emission from fossil fuel burning. *Contemp. Chem. Ind.* **2011**, *40*, 304–306. (In Chinese)
27. Xu, G.; Xu, C.; Yang, Y.; Fang, Y.; Li, Y.; Song, X. A novel flue gas waste heat recovery system for coal-fired ultra-supercritical power plants. *Appl. Therm. Eng.* **2014**, *67*, 240–249. [[CrossRef](#)]
28. Lin, H.; Jin, H.; Gao, L.; Wei, H. Techno-economic evaluation of coal-based polygeneration systems of synthetic fuel and power with CO₂ recovery. *Energy Convers. Manag.* **2011**, *52*, 274–283. [[CrossRef](#)]
29. China Power Engineering Consulting Group Corporation. *Reference Price Index of Thermal Power Engineering Design*; China Electric Power Press: Beijing, China, 2011. (In Chinese)
30. Xu, G.; Yuan, X.; Yang, Y.; Lu, S.; Huang, S.; Zhang, K. Optimization of flue gas desulfurization systems in power plants for energy conservation. *Proc. CSEE* **2012**, *32*, 22–29.
31. Michael, J.M.; Howard, N.S. *Fundamentals of Engineering Thermodynamics*; John Wiley & Sons, Inc.: Hoboken, NJ, USA, 2006.

